International Journal of Mass Spectrometry 345–347 (2013) iv–viii

Contents lists available at ScienceDirect

International Journal of Mass Spectrometry

journal homepage: www.elsevier.com/locate/ijms

Contents

Foreword

1–1
Special Issue Image
2–2
Personal forward
3–4
Personal Forward
5–5
Jennings Biographical Sketch
6–7
Scrivens Biographical Sketch

Regular Articles

8–18

The effect of salt on the conformations of three model proteins is revealed by variable temperature ion mobility mass spectrometry

Yana Berezovskaya, Massimiliano Porrini, Perdita E. Barran

● We examine the effect of sodium iodide on three model proteins using nESI-IM-MS. ● The number of iodides correlates to the number of available basic sites. ● The conformational space occupied by each protein is altered due to the presence of salt and columbic effects. ● Thermally induced unfolding is lessened in the presence of adducted iodide. ● Proteins have lower collision cross sections at 300 K than at 260 K.

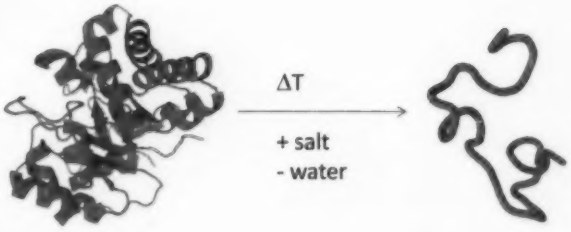

19–27

Localisation of adenine nucleotides in heat-stabilised mouse brains using ion mobility enabled MALDI imaging

Eleanor Q. Blatherwick, Camilla I. Svensson, Bruno G. Frenguelli, James H. Scrivens

● Ion mobility separation improves the selectivity of mass spectrometry imaging. ● Mobility separated MS/MS spectra provide additional confirmatory information. ● Fixing biological tissue prior to imaging studies is essential.

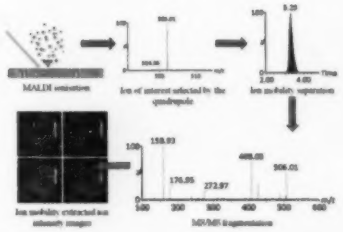

Elsevier B.V.
http://dx.doi.org/10.1016/S1387-3806(13)00198-X

63–70

A tale of a tail: Structural insights into the conformational properties of the polyglutamine protein ataxin-3

Charlotte A. Scarff, Alessandro Sicorello, Ricardo J.L. Tomé, Sandra Macedo-Ribeiro, Alison E. Ashcroft, Sheena E. Radford

● ESI-IMS-MS has been used to characterise ataxin-3 (14Q). ● Ataxin-3 (14Q) shows an array of conformational states. ● The C-terminal domain is largely responsible for its conformational flexibility. ● The dimerisation interface of ataxin-3 is likely to be within the Josephin domain.

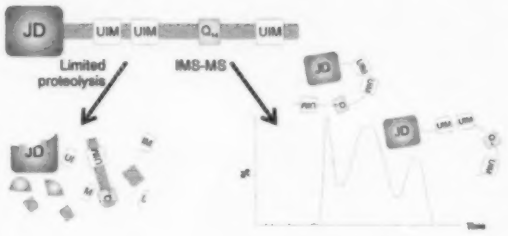

71–79

Fragmentation characteristics of glycopeptides

Károly Vékey, Oliver Ozohanics, Eszter Tóth, Anita Jekő, Ágnes Révész, Judit Krenyácz, László Drahos

● We present energy resolved CID spectra and fragmentation characteristics of glycopeptides. ● We suggest that glycopeptide analysis should be performed at low energy (SY50) to maximize information content. ● Possibility to determine fucosylation site based on MS/MS.

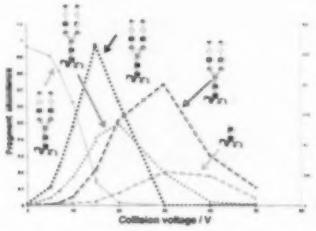

80–88

Hydrocarbon analysis using desorption atmospheric pressure chemical ionization

Fred P.M. Jjunju, Abraham K. Badu-Tawiah, Anyin Li, Santosh Soparawalla, Iman S. Roqan, R. Graham Cooks

● Analysis of petroleum constituents is achieved under ambient conditions. ● Proton or electron transfer reactions are carried out under ambient conditions. ● Charge exchange using naphthalene as the DAPCI reagent gave simple mass spectra consisting of only molecular cation $M^{+\bullet}$ without side products. ● Unleaded gasoline and diesel standard mixtures can be characterized.

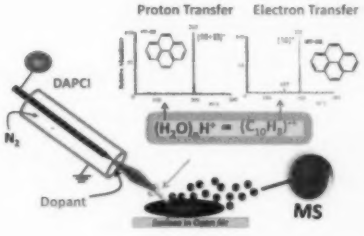

89–96

A novel projection approximation algorithm for the fast and accurate computation of molecular collision cross sections (II). Model parameterization and definition of empirical shape factors for proteins

Christian Bleiholder, Stephanie Contreras, Thanh D. Do, Michael T. Bowers

● We derive atomic parameters for use with the projected superposition approximation (PSA). ● We apply the PSA method to 396 protein structures from the Protein Data Bank with up to 300 kDa in weight. ● We define an empirical shape factor to estimate the PSA cross section for proteins. ● The empirical shape factor is accurate to approximately 10%.

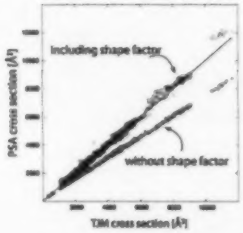

97–103

Thermal dissociation of streptavidin homotetramer in the gas phase: Subunit loss versus backbone fragmentation

Elena N. Kitova, Igor Sinelnikov, Lu Deng, John S. Klassen

● Thermal dissociation pathways of gas phase protonated ions of the homotetramer streptavidin are elucidated. ● Backbone fragmentation and water loss compete with the loss of intact subunit. ● Kinetic data consistent with the presence of multiple non-interconverting structures. ● Proposed that backbone fragmentation requires unfolding of the N-terminus of the subunit.

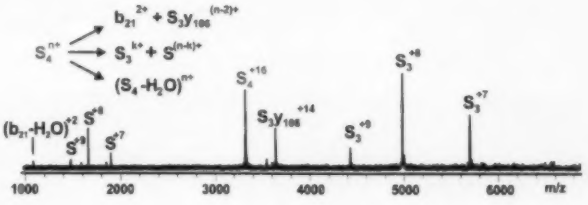

104–108

Selective solvent extraction and characterization of the acid extractable fraction of Athabasca oils sands process waters by Orbitrap mass spectrometry

J.V. Headley, K.M. Peru, B. Fahlman, A. Colodey, D.W. McMartin

● Negative-ion electrospray Orbitrap MS is well suited for the characterization of NAs and NAFCs in Athabasca OSPW. ● For comparison of results from a given sample set it is critical to consider solvent extraction effects. ● A routine monitoring program concerned only with the O_2 species may choose hexane as the extraction solvent as it provides a more selective extraction of these species. ● On the other hand, using ENV+ (SPE) provides less selective extraction better suited for full characterization of a sample.

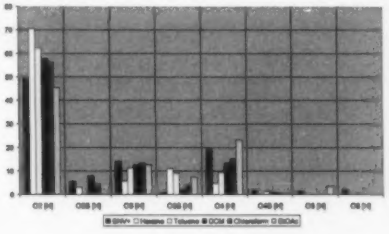

109–119

Role of methylation on the thermochemistry of alkali metal cation complexes of amino acids: N-methyl proline

Abhigya Mookherjee, P.B. Armentrout

● Energy-resolved CID of alkali cation complexes of N-methyl proline are studied using guided ion beam tandem mass spectrometry. ● Threshold CID data are analyzed to yield absolute bond energies for M⁺(N-methyl proline) where M = Li, Na, K, and Rb. ● Quantum chemical calculations explore the possible conformations of N-methyl proline and its alkali metal cation complexes. ● Agreement between experimental and theoretical bond energies show that M⁺(N-methyl proline) have zwitterionic structures.

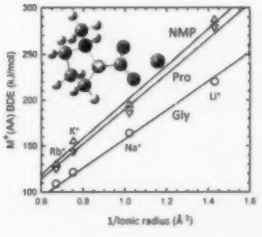

120–131

Mass spectra of halogenostyrylbenzoxazoles

Stephen T. Ayrton, Jekaterina Panova, Adam R. Michalik, William H.C. Martin, Richard T. Gallagher, Richard D. Bowen

● 5-Halogenostyrybenzoxazoles (SBOs) show strong $[M-H]^+$ peaks in their EI mass spectra. ● Strong $[M-Y]^+$ signals occur in the spectra of ortho substituted SBOs. ● The strong $[M-H]^+$ and $[M-Y]^+$ signals can be attributed to a proximity effect. ● Loss of F• by the proximity effect preempts loss of Br• from the benzoxazole ring. ● Ortho substituted SBOs can be easily distinguished from their meta and para isomers.

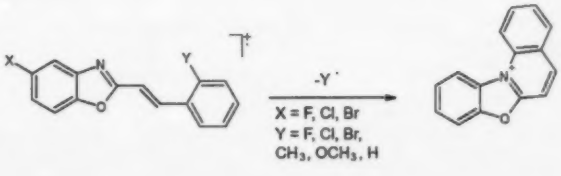

132–141

Lysine hydroxylation and O-glycosylation in the globular, C-terminal region of mammalian-expressed, recombinant PrP

Mark A. Ritchie, Lawrence G. Hunt, Andrew C. Gill

● Recombinant, mammalian-expressed prion protein contains a modification in the C-terminal domain. ● Lys193 is converted to hydroxylysine with a disaccharide added to the new hydroxyl. ● Mass spectrometry and Edman degradation demonstrate the presence of the modification. ● Molecular dynamics indicates that lys193 glycans produce stabilisation of a critical loop of PrP.

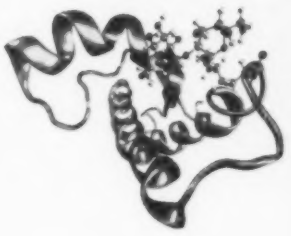

142–152

Dissociations of gas-phase complexes of deprotonated glutathione with Co^{2+}, Ni^{2+}, Cu^{2+} and Zn^{2+}: The importance of metal ion reduction

Laura Banu, Voislav Blagojevic, Diethard K. Bohme

● We electrosprayed 1:1 complexes of deprotonated glutathione $(GSH-H)^-$, and the metal dications Co^{2+}, Ni^{2+}, Cu^{2+} and Zn^{2+}. ● Both positive, $[M(GSH-H)]^+$, and negative, $[M(GSH-3H)]^-$, complexes were observed, where M is the transition metal. ● These metal complexes, $[M(GSH-H)]^+$, and bare $(GSH-H)^-$ were exposed to multi-collisional dissociation (CID). ● CID of complexes with M = Co, Ni, Zn found to be similar to CID $(GSH-H)^-$, so M^{2+} binds at cysteine with ligand mostly unchanged. ● Unique CID of Cu^{2+} complexes was attributed to ligand radical structures formed by the reduction of intra-complex

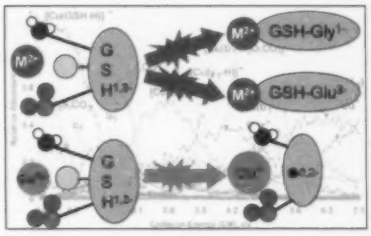

153–159

Charge detection mass spectrometry for single ions with a limit of detection of 30 charges

Nathan C. Contino, Martin F. Jarrold

● A new charge detection mass spectrometer is described. ● Ions are energy selected prior to entering a cone trap with an image charge detector. ● A limit of detection of 30 elementary charges is achieved. ● The average uncertainty in the charge measurements is 3.2 elementary charges. ● Mass distributions measured for BSA (66.4 kDa) show monomer and multimer ions.

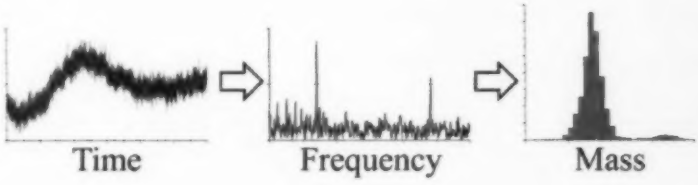

160–166

Reprint of "Binding energies determined from kinetic energy release measurements following the evaporation of single molecules from the molecular clusters $H^+(H_2O)_n$, $H^+(NH_3)_n$ and $H^+(CH_3OH)_n$"

E. Bruzzie, R. Parajuli, A.J. Stace
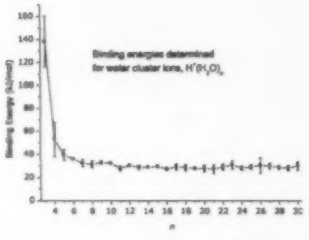
● Kinetic energy releases recorded for $H^+(H_2O)_n$, $H^+(NH_3)_n$ and $H+(CH_3OH)_n$ clusters. ● Results trans-formed into binding energies using finite heat bath theory. ● Results show a quantitative agreement with the strengths of hydrogen bonds. ● Concluded that each cluster fragments via the breaking of asingle hydrogen bond.